On the thickness of discontinuities computed by THINC and RK schemes

○ Taku Nonomura, ISAS, JAXA, Sagamihara, Kanagawa, Japan, E-mail:nonomura@flab.isas.jaxa.jp
Keh-Ming Shyue, National Taiwan University, Tapei, Taiwan

In this study, the thickness of discontinuities computed by tangent hyperbola interpolation for interface capturing (THINC) and Runge-Kutta (RK) schemes are investigated using a linear advection equation. First, characteristics of two variants of the THINC scheme are investigated: one is modified THINC scheme the maximum and minimum of hyperbolic tangent of which are based on neighbor cell and the other is original THINC scheme the maximum and minimum of hyperbolic tangent of which are fixed to be 1 and 0, respectively. The results show that the thickness fo discontinuity of the modified THINC scheme is far from the targeted one and one of the original THINC scheme agrees well with the target one, when the target thickness is smooth. On the other hand, the thickness of both schemes are almost the same and becomes slightly smoother than targeted one, when the target thickness is sharp. This illustrates the accuracy of the modified THINC scheme is acceptable for the practical simulations in which the sharper interface is given. Then, characteristics of THINC and RK schemes with various CFL number are investigated. When the odd-number-stage RK schemes investigated in this study are adopted with the CFL number of higher than the certain value, the overshoots are observed. On the other hand, such overshoots do not appear when the even-number-stage RK schemes investigated in this study are adopted. These result illustrate that we should take care of kinds of RK schemes and CFL numbers, to avoid the overshoot and realize the robust computation.

1. Introduction

Recently, various two-phase flow computations are conducted. There are two ways to treat the interface of two-phase flows: interface capturing and interface tracking methods. Here, interface capturing methods employ a smoothed (diffused) interface on the grid points, while the tracking methods adopt the sharp interface across the grid points. A volume of fluid (VOF) method is usually categorized into interface capturing methods. Thus far, the interface is computed with piecewise-linear-interface-calculation (PLIC) methods or its variants in the VOF methods.

Although the PLIC method or its variants work well for capturing sharp interface, their procedure is relatively complicated. Therefore, alternative simpler methods have been proposed and improved. One of them is a tangent hyperbola for interface capturing (THINC) scheme.[1] In the THINC scheme, advection equation of the volume fraction is solved with the reconstruction based on the hyperbolic tangent function. The THINC scheme has been modified[2-4] and applied to various problems.

One of the applications of the THINC scheme is compressible two-phase flow.[5,6] Thus far, the THINC scheme is applied to the five equation formulation[6] and the two-fluid modeling.[5] In the compressible two-phase flow simulation, the more robust variant of the THINC scheme is sometimes used for the compressible fluid simulations in which the minimum and maximum of hyperbolic tangent function is set to be minimum and maximum of neighbor cells. The characteristics of this variant has not also been clarified. Also, in the compressible two-phase flow simulation, the volume fraction is not conserved and usually solved with the Runge-Kutta time integration method, though the formulation for the incompressible flow on the structured mesh is sometimes solved by exact time integration method with the Strang type dimension-by-dimension splitting by assuming the conservation of volume. However, the characteristics of the THINC scheme combined with the RK scheme have not been clarified with changing the CFL number.

In this presentation, for the future compressible two-phase flow simulations, two characteristics above are investigated: 1) effects of a robust implementation of the THINC scheme and 2) effects of the CFL number or choice of RK schemes on THINC and RK schemes. These effects are investigated by using the one-dimensional linear advection equation.

2. Formulation and Metrics

In this paper, following linear advection equations are solved by THINC and RK schemes:

$$\frac{\partial u}{\partial t} + \frac{\partial f}{\partial x} = 0, \tag{1}$$

$$f = u. \tag{2}$$

Here, the initial condition is set to be

$$u = \begin{cases} 0 & 0.25 \le x \le 0.75 \\ 1 & otherwise \end{cases} \tag{3}$$

with the computational domain of $0 \le x < 1$ and periodic boundary conditions.

A finite volume method is used for the discretization. The semidiscretized form of equation (1) is as follows:

$$\frac{\partial \bar{u}_j}{\partial t} = R_j \tag{4}$$

$$R_j = -\frac{1}{\Delta x} \left(f_{j+1/2} - f_{j-1/2} \right), \tag{5}$$

where $\bar{u}_j$ is the discretized cell-averaged quantity on the jth grid point and $f_{j+1/2}$ is the numerical flux and is given by the following equation:

$$f = u_L. \tag{6}$$

Here, u_L is interpolated variable on the left side of cell edge. In the original THINC scheme it is computed as follows. First, the distribution of u in the cell is reconstructed by the hyperbolic tangent function.

$$u(x) = \frac{1}{2} \left(1 + \tanh(\beta(aX + d)) \right), \tag{7}$$

$$X = \frac{x - x_{j-1/2}}{x_{j+1/2} - x_{j-1/2}}, \tag{8}$$

where a is determined by the gradient of the volume fraction and b is determined to adjust the cell average of the hyperbolic tangent function to the given $\bar{u}$. The calculation formula of a and b for the given profile is
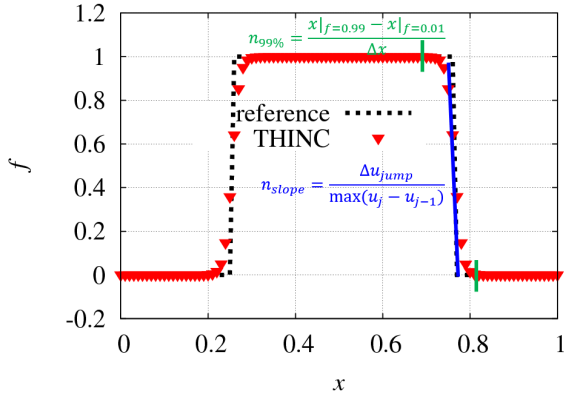
Fig. 1: Schematic of discontinuity thickness.

Fig. 2: Ideal values of discontinuity thickness for assumed profiles.

described in the reference.[3,5] Here, β is the parameter which determines the sharpness of the interface: Larger β gives the sharper interface as shown later. It should be note that the hyperbolic tangent function with minimum of 0 and maximum of unity is used for the original THINC scheme.

As noted in the introduction, in the modified robust THINC scheme, the minimum and maximum values of hyperbolic tangent function are set to be those of neighbor cells. In this case, Eq. 9 is modified as follows:

$$u(x) = u_{\min} + \frac{u_{\max} - u_{\min}}{2}\left(1 + \tanh(\beta(aX + d))\right), \tag{9}$$

$$u_{\min} = \min(u_{j-1}, u_{j+1}), \tag{10}$$

$$u_{\max} = \max(u_{j-1}, u_{j+1}). \tag{11}$$

In this case, the monotonicity of the interpolated variables are maintained and the robustness is improved.[6,7]

With regard to the time advancement, the Euler explicit, Runge-Kutta and exact time integration schemes are used.

Then, the metrics for evaluation of results are defined here. First, the discontinuity thickness is used for the metrics of sharpness of the interface. In this paper, two kinds of discontinuity thickness are introduced. One is slope-based thickness, and the other is 99%-based thickness. Here, the slope-based thickness is defined as follows:

$$n_{slope} = \frac{\Delta u_{jump}}{\max(|u_j - u_{j+1}|)}, \tag{12}$$

where the discontinuity jump Δf_{jump} is set to be unity in this problem. On the other hand, the 99%-based thickness is defined as follows:

$$n_{99\%} = \frac{1}{\Delta x}\left(x\big|_{\frac{u-u_{\min}}{\Delta u_{jump}}=0.01} - x\big|_{\frac{u-u_{\min}}{\Delta u_{jump}}=0.99}\right). \tag{13}$$

Here, $u_{\min}$ is minimum value of the initial condition which is set to be 0 in this problem. A schematic of these discontinuities is shown in Fig. 1. If the exact hyperbolic tangent distribution is assumed, the discontinuities are functions of only the one parameter β in the hyperbolic tangent function as shown in Fig. 2.

In addition to the sharpness of the interface, the robustness is important for the kinds of multiphase flow
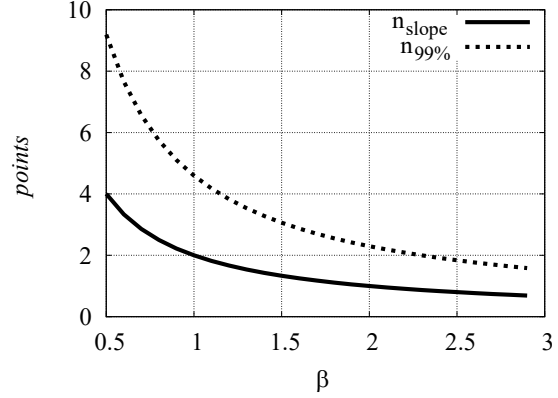
simulation. The computation often fails when the negative volume fraction appears. In order to avoid such a situation, the overshoot and the undershoot should be prevented. Therefore, the percentage of the overshoot are used for the metrics of the robustness, whereas the percentage of the undershoot of this problem is exactly the same as that of overshoot. The zero percent of the overshoot are preferred for the robust simulations.

Those metrics are measured during the duration $1 < t < 2$, in which the discontinuities make second round and the distribution becomes almost in the quasi-steady state. The discontinuity thicknesses are obtained by taking the average in the duration, while the overshoot is evaluated by taking the maximum.

3. Comparison of Original and Modified Robust THINC Schemes

In this section, the discontinuities computed by the original and modified robust THINC schemes are discussed. Because the CFL number and choice of RK schemes affect the results for the larger-CFL-number condition as discussed later in the next section, we use the two-stage second-order SSP RK scheme with the CFL number of 0.1 which is sufficiently small for obtaining the CFL number independent solution.

In these condition, no overshoots are observed owing to the smaller CFL number. Therefore, the only discontinuity thickness is discussed here. Fig. 3 shows the discontinuities computed by the two THINC schemes, together with the ideal values based on the assumed profile. For both discontinuities, the discontinuities of the modified robust THINC scheme becomes much thicker than those of original one, which is close to the ideal values based on the assumed profile, for smaller β condition ($\beta < 1.8$), i.e. the much diffused condition. On the other hand, the clear differences are not observed for larger β condition ($\beta > 1.8$) in which the discontinuities of both original and modified robust THINC schemes have discrepancies from the ideal values based on the assumed profile. This results suggest that the discontinuities computed by the modified robust THINC scheme are different from the assumed profile in the condition in which the discontinuities are captured with sufficient points, while the modified robust THINC scheme works as well as original scheme in the condition in which the discontinuities are captured with a few points as in the practical simulations. This implies the modified robust THINC scheme seems to be a good candidate for the practical simulations.
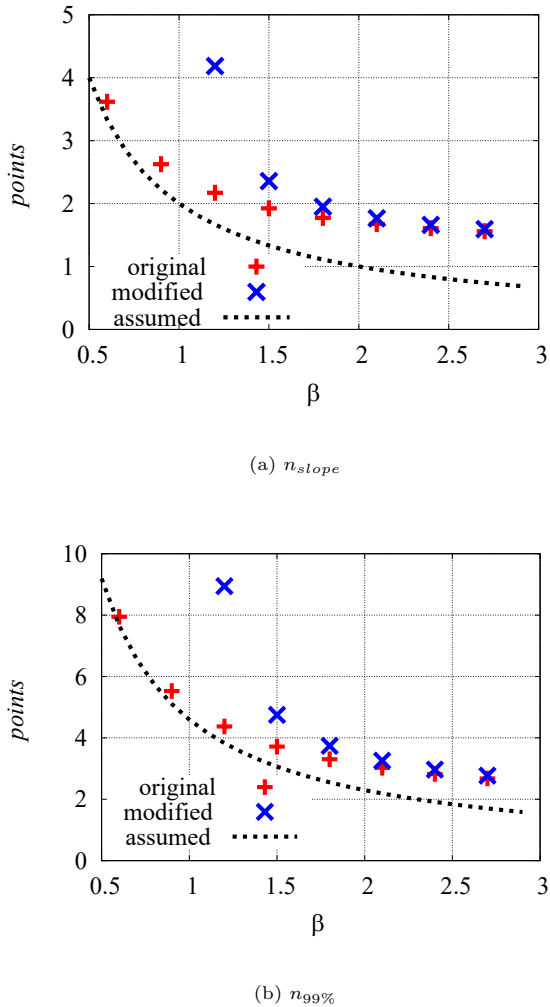
(a) Euler explicit scheme

(b) three-stage thidr-order SSP RK scheme

Fig. 4: Overshoots for various RK schemes and CFL numbers.

(a) n_{slope}

(b) $n_{99\%}$

Fig. 3: Discontinuity thickness for various β of original and modified THINC schemes.

4. Comparison of THINC and RK Schemes with Various CFL numbers

In this section, the effects of the CFL number and choice of RK schemes on the discontinuities computed by the original THINC schemes combined by the RK time-advancement schemes. In the series of tests, we set $1.5 \leq \beta \leq 2.7$ with CFL numbers of 0.1, 0.2, 0.3, 0.4, 0.5, and 0.6 for each scheme: Euler, two-stage second-order SSP, three-stage third order SSP schemes and exact time integration.

First, the overshoot characteristics are discussed. Interestingly, we do not have any overshoot in the two-stage second-order SSP RK scheme and exact time integration. This characteristic is also observed in the four-stage second-order SSP RK scheme which is not shown for brevity and the results implies that the even-number-stage SSP RK scheme might not have any overshoot. On the other hand, results of the odd-number-stage SSP RK scheme are shown in Fig. 4. Results show that the overshoot is observed for the Euler explicit scheme with the CFL number of larger than 0.25 and for the three-stage third-order SSP RK scheme with the CFL number of larger than 0.4. This results suggest that the CFL number should be carefully chosen for the odd-number-stage SSP RK schemes.

Then, the discontinuity thickness is discussed. The results for two discontinuity thicknesses are shown in Figs 5 and 6. Interestingly, the discontinuity thickness becomes larger with increasing the CFL number for the two-stage second-order SSP RK scheme, while it becomes smaller with increasing CFL number for the three-stage third-order SSP RK scheme. Meanwhile, the discontinuity thickness of the exact time integration does have strong dependency on the CFL number. Here, the Euler explicit scheme have similar characteristics to the three-stage third order SSP RK scheme, though we do not show the results for the Euler explicit scheme for the brevity. These result suggest that the Euler explicit and three-stage third order SSP RK schemes (i.e. maybe even-number-stage SSP-RK schemes) have the characteristics that the discontinuity becomes sharper with increasing the CFL number and it causes the overshoot characteristics of those scheme in the larger CFL number condition owing to the sharper discontinuities.

5. Conclusions

In this study, the thickness of discontinuities computed by tangent hyperbola interpolation for interface capturing (THINC) and Runge-Kutta (RK) schemes are investigated using a linear advection equation. First, characteristics of two variants of the THINC scheme are investigated: one is modified THINC scheme the maximum and minimum of hyperbolic tangent of which are based on neighbor cell and the other is original THINC scheme the maximum and minimum of hyperbolic tangent of which are fixed to be 1 and 0, respectively. The results show that the thickness fo discontinuity of the modified THINC scheme is far from the targeted one and one of the original THINC scheme agrees well with the target one, when the target thickness is smooth. On the other hand, the thickness of both schemes are almost the same and becomes slightly smoother than targeted one, when the target thickness is sharp. This illustrates the accuracy of the modified THINC scheme is acceptable for the practical simulations in which the sharper interface is given. Then, characteristics of THINC and RK schemes with various CFL number are investigated. When the odd-number-stage RK schemes investigated in this study are adopted with the CFL number of higher than the certain value, the overshoots are observed. On the other hand, such overshoots do not appear when the even-number-stage RK schemes investigated in this study are adopted. These result illustrate that we should take care of kinds of RK schemes and CFL numbers, to avoid the overshoot and realize the robust computation.

Acknowledgment

References

(1) Xiao, F. and Honma, Y., and Kono, T., "A simple algebraic interface capturing scheme using hyperbolic tangent function," Int. J. Num. F, 48 (2003), pp. 1023-1040.

(2) Xiao, F., Ii, S. and Chen, C., "Revisit to the THINC scheme: A simple algebraic VOF algorithm," J. Comp. Phys., 230 (2011), pp. 7086-7092.

(3) Ii, S., Sugiyama, K., Takeuchi, S., Takagi, S., Matsumoto, Y. and Xiao, F., "An interface capturing method with a continuous function: The THINC method with multi-dimensional reconstruction," J. Comp. Phys., 231 (2011), pp. 2328-2358.
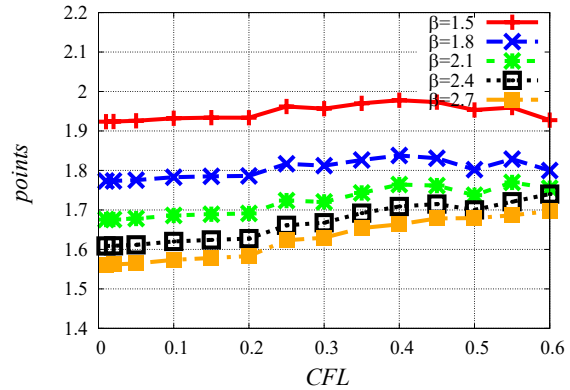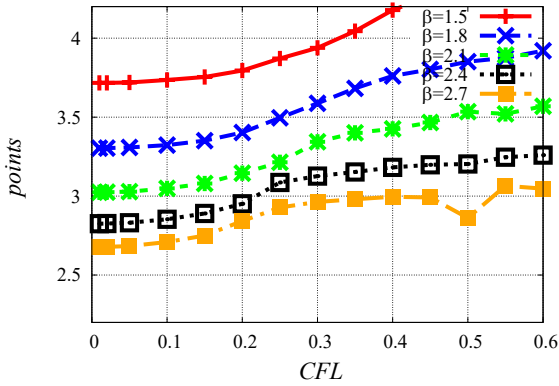

(a) two-stage second-order SSP RK scheme
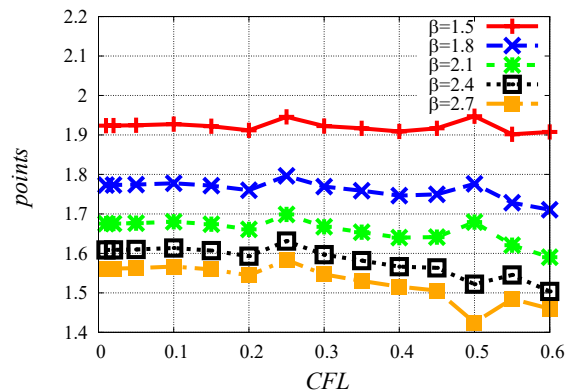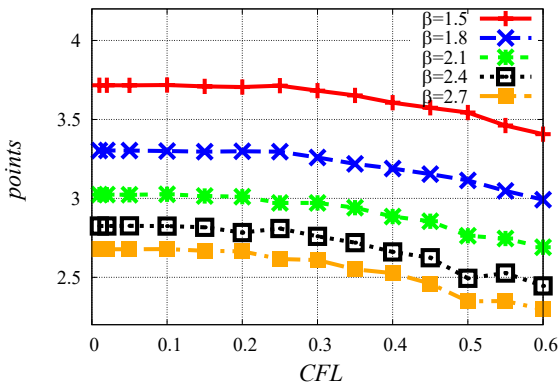

(b) three-stage third-order SSP RK scheme
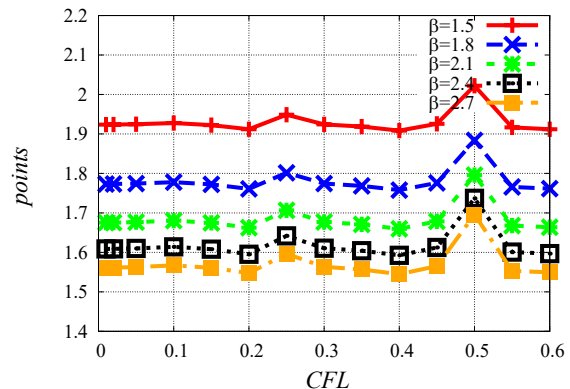
(c) theoritical time integaration

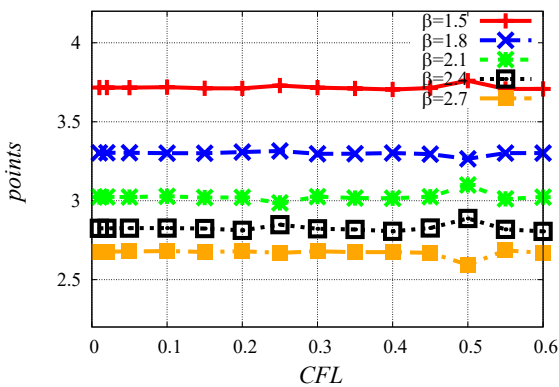Fig. 5: n_{slope} for various RK schemes and CFL numbers.

(4) Ii, S., Bin, X., Xiao, F., "An interface capturing method with a continuous function: The THINC method on unstructured triangular and tetrahedral meshes," J. Comp. Phys., 259 (2014), pp. 260-269.

(5) Nonomura, T., Kitamura, K., Fujii, K., "A simple interface sharpening technique with a hyperbolic tangent function applied to compressible two-fluid modeling," J. Comp. Phys., 258 (2014), pp. 95-117.

(6) Shyue K.M. and Xiao F., "An Eulerian interface sharpening algorithm for compressible two-phase flow: The algebraic THINC approach," J. Comp. Phys., 268 (2014), pp. 326-354.

(7) Sumi T. and Kurotaki T., "Numerical Solution with High-order Accuracy and High Resolution for Compressible Multiphase Flows based on Diffuse Interface Model," 28th CFD Symp. in Japan, (2014), C05-2.

(a) two-stage second-order SSP RK scheme

(b) three-stage third-order SSP RK scheme

(c) theoritical time integaration

Fig. 6: $n_{99\%}$ for various RK schemes and CFL numbers.